1 **Using 3D geometric morphometrics to aid taxonomic and ecological understanding of**

2 **a recent speciation event within a small Australian marsupial (genus *Antechinus*)**

3 Pietro Viacava[1], Andrew M. Baker[2,3], Simone P. Blomberg[1], Matthew J. Phillips[2] and
4 Vera Weisbecker[4]

5 [1]School of Biological Sciences, The University of Queensland, St Lucia, Queensland, Australia

6 [2]School of Biology and Environmental Science, Queensland University of Technology, Brisbane,
7 Queensland, Australia

8 [3]Natural Environments Program, Queensland Museum, PO Box, 3300, South Brisbane, QLD 4101,
9 Australia

10 [4]College of Science and Engineering, Flinders University, Adelaide, South Australia, Australia

11

12 **Abstract**

13 Taxonomic distinction of species forms the foundation of biodiversity assessments and

14 conservation priorities. However, traditional morphological and/or genetics-based taxonomic

15 assessments frequently miss the opportunity of elaborating on the ecological and functional

16 context of species diversification. Here, we used 3D geometric morphometrics of the cranium

17 to improve taxonomic differentiation and add eco-morphological characterisation of a young

18 cryptic divergence within the marsupial carnivorous genus *Antechinus*. Specifically, we used

19 168 museum specimens to characterise the recently proposed clades *A. stuartii* "south", *A.*

20 *stuartii* "north" and *A. subtropicus*. Beyond slight differences attributable to overall size (and

21 therefore not necessarily diagnostic), we also found clear allometry-independent shape

22 variation. This allowed us to define new, easily measured diagnostic traits in the palate, which

23 differentiate the three clades. Contrary to previous suggestions, we found no support for a

24 latitudinal gradient as causing the differentiation between the clades. However, skull shape

25 co-varied with temperature and precipitation seasonality, suggesting that the clades may be

26 adapted to environmental variables that are likely to be impacted by climate change. Our study

27 demonstrates the use of 3D geometric morphometrics to improve taxonomic diagnosis of

28 cryptic mammalian species, while providing perspectives on the adaptive origins and potential

29 future threats of mammalian diversity.

30 **Keywords:** antechinus ecology - antechinus taxonomy - conservation - cryptic species –

31 ecomorphology - geometric morphometrics - Procrustes ANOVA - shape variation - variation

32 partitioning

33 **I. Introduction**

34   Mammalian biodiversity is globally under threat due to anthropogenic impacts, which

35 include changing patterns of temperature and rainfall, and increased frequency and duration

36 of extreme bushfires (Bowman *et al.*, 2020). In terms of species loss, the Australian

37 mammalian fauna is globally the most affected due to widespread environmental degradation

38 (Woinarski, Burbidge, & Harrison, 2015) from introduced species, agriculture, logging and

39 extreme vegetation fire events (Pardon *et al.*, 2003; Letnic, Tamayo, & Dickman, 2005; Firth

40 *et al.*, 2010; Pastro, 2013; Crowther *et al.*, 2018; Radford *et al.*, 2018; Murphy *et al.*, 2019).

41 Furthermore, Australia is predicted to endure increasingly frequent fire-weather and extreme

42 droughts (Di Virgilio *et al.*, 2019; Dowdy *et al.*, 2019; Ukkola *et al.*, 2020; Kirono *et al.*, 2020).

43 The east coast of Australia is particularly vulnerable in terms of biodiversity loss: the 2019-

44 2020 mega-fires of south-eastern Australia destroyed habitat within the distribution of 832

45 vertebrate taxa, of which 83 were mammalian species (Ward *et al.*, 2020). Hence, the

46 implementation of widespread conservation efforts for over one hundred threatened Australian

47 mammal species is a high priority (Legge *et al.*, 2018).

48   The planning of such conservation efforts relies on a good understanding of what

49 species inhabit the most affected environments. However, the advent of modern molecular

50 methods is driving the discovery of previously unrecognized "cryptic" species and is

51 increasingly pointing towards unexpectedly high biodiversity losses, with taxa at risk of

52 extinction shortly after, or even before, discovery (May, 1988; Dubois, 2003). This particularly

53 affects many species that are considered to be "known" but may eventually undergo taxonomic

54 revision with the development of more accurate taxonomic methods (Bickford *et al.*, 2007;

55 Chaplin *et al.*, 2020). Thus, we may be underestimating well-studied species initially classified

2

56   as not threatened that may instead contain evolutionary lineages sufficiently distinct to deserve

57   re-examination of their conservation status.

58   The issue of unrecognised biodiversity goes beyond the fundamental question of how

59   many species exist. Characterising the phenotypic diversity in closely related species is also

60   essential for understanding their interaction with the environment – that molecular data alone

61   does not provide – and the reason for the species divergence. However, the phenotypic

62   diversity in young species is generally measured using well-established morphological

63   diagnostics (e.g., Baker, Mutton, & Van Dyck, 2012; Baker *et al.*, 2012; Baker, Mutton, &

64   Hines, 2013) that were designed with a view to species differentiation, rather than the

65   processes that may have led to phenotypic divergence. In order to identify conservation units

66   worthy of protection, we need to understand the ecological processes that may lead to species

67   diversification – in fact, ecological exchangeability is a defining factor of Evolutionary

68   Significant Units (Crandall *et al.*, 2000; Fraser & Bernatchez, 2001; de Guia & Saitoh, 2007).

69   In particular, population divergence and speciation is widely known to occur in association with

70   certain ecological boundaries. For example, in coastal eastern Australia, the Brisbane Valley

71   represents a biogeographic break (Bryant & Krosch, 2016) for divergence of arthropods

72   (Lucky, 2011; Rix & Harvey, 2012), reptiles (Chapple, Chapple, & Thompson, 2011a; Chapple

73   *et al.*, 2011b), amphibians (McGuigan *et al.*, 1998; James & Moritz, 2000) and mammals

74   (Bryant & Fuller, 2014); the Clarence River Corridor (Bryant & Krosch, 2016) is also known

75   for the divergence of reptiles (Colgan, O'Meally, & Sadlier, 2010) and mammals (Rowe *et al.*,

76   2012; Frankham, Handasyde, & Eldridge, 2012). Thus, assessing the ecological interaction

77   and the distribution of morphologically diversified vertebrate taxa, particularly across

78   biogeographic breaks, is key to understanding the role of biotic and abiotic factors in the

79   divergence of these species.

80   The marsupial mammal genus *Antechinus* (MacLeay, 1841) is a case in point of

81   unrecognised diversity located on the Australian east coast. Antechinuses are small,

82   scansorial and insectivorous marsupials (Lee & Cockburn, 1985), which play an important role

3

83   as pollinators (Goldingay, Carthew, & Whelan, 1991; Goldingay, 2000). The genus also

84   displays the unusual trait of semelparity, where all males die after an annual 1-3 week mating

85   period (Kraaijeveld- Smit, Ward, & Temple- Smith, 2003; Holleley *et al.*, 2006; Fisher *et al.*,

86   2013). Antechinuses are also predicted to be particularly susceptible to changes in rainfall

87   patterns: members of this genus synchronize their only mating event in the life of a male with

88   rainfall-dependant peaks of insect abundance (Fisher *et al.*, 2013).   .

89   Antechinus species are a good example of accelerated biodiversity recovery in the wake

90   of recent advances in molecular biology (Baker & Dickman, 2018). Several species in the

91   genus have recently been taxonomically re-described and others have been discovered,

92   expanding their known diversity from 10 to 15 species since 2012 (Baker *et al.*, 2012, 2013,

93   2014, 2015; Baker & Van Dyck, 2013a,b,c, 2015), with two of these classified as federally

94   Endangered (*Antechinus arktos* and *Antechinus argentus*) (EPBC Act, 1999; Geyle *et al.*,

95   2018).

96   The species complex *Antechinus stuartii* has been a focus of taxonomic change since its

97   description by MacLeay in 1841. Five species are currently recognized to have been once part

98   of *A. stuartii* (*sensu lato*): *Antechinus flavipes* (Waterhouse, 1837) (see in Baker & Van Dyck,

99   2013b); *Antechinus adustus* (Thomas, 1923) (see in Van Dyck & Crowther, 2000); *Antechinus*

100   *agilis* Dickman *et al.*, 1998, *Antechinus subtropicus* Van Dyck & Crowther, 2000 and *A. stuartii*

101   MacLeay, 1841 (*sensu stricto*; see in Jackson & Groves, 2015). Notably, the difficulties with

102   taxonomic resolution have been driven by a lack of phenotypic differentiation; for instance, *A.*

103   *stuartii* and *A. agilis* were still thought to be morphologically cryptic until near the end of the

104   century (Sumner & Dickman, 1998). Further taxonomic clarification of *A. stuartii* has recently

105   been recommended after genetic studies revealed multiple lineages (Mutton *et al.*, 2019).

106   Previous traditional morphological work (including linear measurements and discrete

107   characters) found a subtle differentiation between *A. subtropicus* and *A. stuartii*, particularly in

108   cranial size, rostral proportions and palatal morphology (Van Dyck & Crowther, 2000),

109   although the morphological differences were not clearly defined. However, subsequent

4

110   molecular work (Mutton *et al.*, 2019) suggested that *A. stuartii* contains two lineages and is

111   paraphyletic: *A. subtropicus* and an *A. stuartii* north clade appear genetically more closely

112   related to the exclusion of the *A. stuartii* south clade (Figure 1). These taxa have apparently

113   arisen from a recent speciation event dated from the Pleistocene (~ 2 Mya) (Mutton *et al.*,

114   2019). Further morphological evidence is therefore required to assess the taxonomy of the

115   northern and southern *A. stuartii* clades and to examine the relationship of both these taxa

116   with *A. subtropicus.*
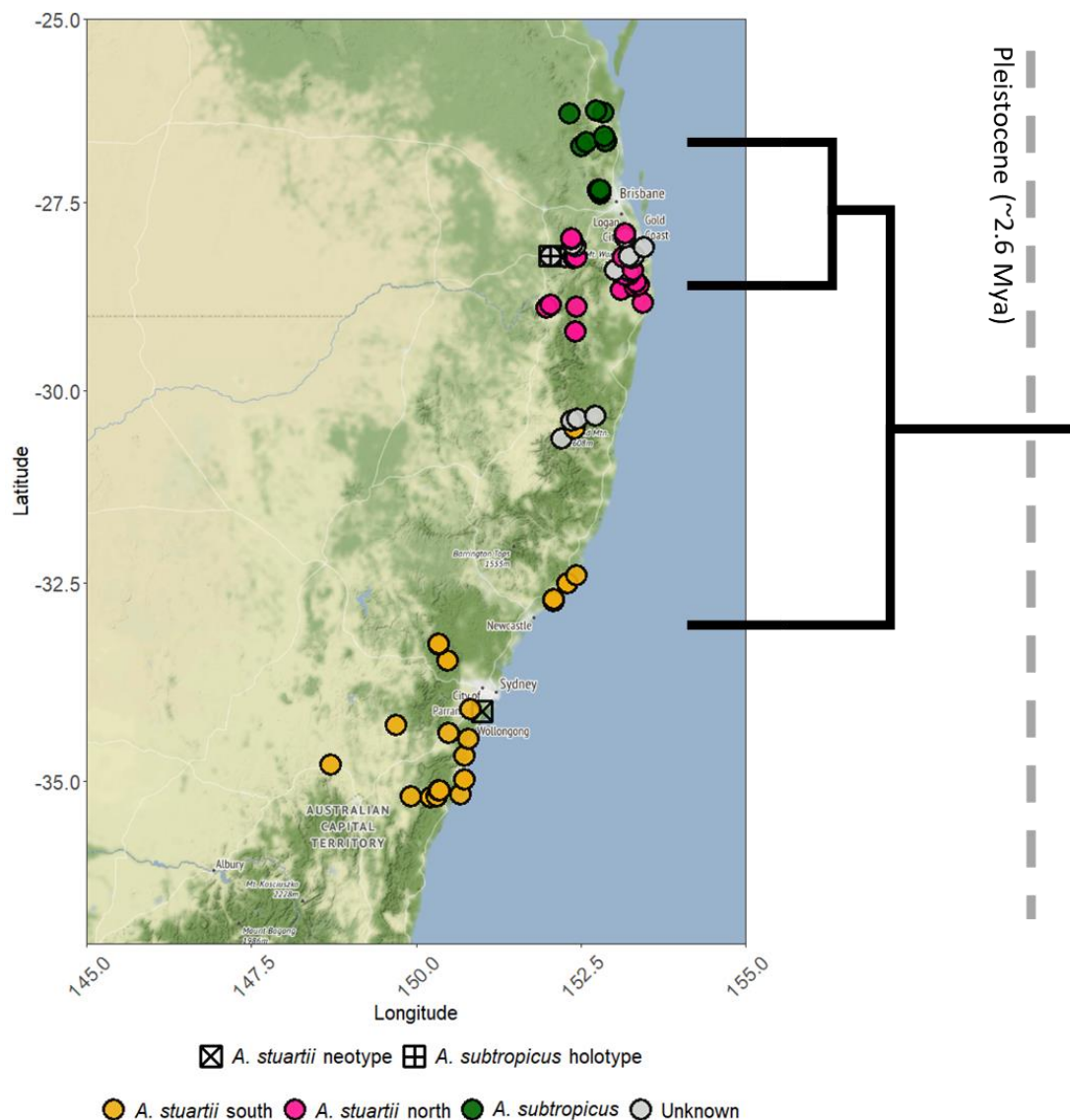
117

118   **Figure 1:** Distribution map of the specimens used for this study. Labelled are A. stuartii south,
119   A. stuartii north, A. subtropicus, specimens of unknown identity within the A. stuartii - A.
120   subtropicus species complex, the holotype of A. subtropicus and the neotype of A. stuartii. All
121   figures in this paper are labelled: A. stuartii south in orange, A. stuartii north in pink and A.
122   subtropicus in green. The phylogeny is adapted from Mutton et al. (2019).

5

123   The *Antechinus stuartii* species complex presents a unique opportunity to assess

124   morphological differentiation at the boundaries of a complex of young, closely related species.

125   Because they apparently occur along a latitudinal cline, the *A. stuartii* complex also provides

126   the context for an assessment of ecological and geographic factors that drive species

127   differentiation and are the chief predictors of future species distributions. In this study, we take

128   advantage of 3D geometric morphometrics to investigate the morphological diversification

129   within the *A. stuartii – A. subtropicus* complex. The benefit of geometric morphometrics over

130   conventional morphological measurements in this context is that it allows a global assessment

131   of shape retained through variation and differentiation analyses, with graphical depictions

132   permitting accurate biological interpretations (Adams, Rohlf, & Slice, 2013). We therefore aim

133   to: a) test for corroboration of the genetically known clades with dependable morphological

134   differentiators (taxonomic aspect); b) evaluate the environmental drivers associated within and

135   between clades (ecomorphological aspect); and c) infer an evolutionary hypothesis for the

136   speciation events (evolutionary aspect).

137   **II.   Material and methods**

138   **a) *Data collection***

139   Our study included 168 3D models of adult individuals (determined by complete P3

140   premolar tooth eruption). These included specimens of *Antechinus subtropicus* (n = 68; 41

141   males, 25 females and 2 of unknown sex), *Antechinus stuartii* north (n = 30; 16 males, 12

142   females and 2 of unknown sex), *Antechinus stuartii* south (n = 38; 15 males, 22 females and

143   1 of unknown sex) and *A. subtropicus / A. stuartii* where clades were unassigned (n = 32; 19

144   males, 8 females and 5 of unknown sex). To determine clade groupings, first, specimens were

145   assigned a species (*A. subtropicus* or *A. stuartii*) following identification by museum curators.

146   Second, we corroborated this information with specimens that were assigned a clade

147   genetically in the literature. Third, we assigned the remaining specimens following the

148   presumed distribution of the clades, as they are largely geographically non-overlapping

149   (Mutton *et al.*, 2019). To assign *A. stuartii* specimens to the northern or southern lineage, we

6

150   relied on the locality in which they were captured (the lineages are largely geographically non-

151   overlapping, with a narrow zone of sympatry) and genetic analyses (two mtDNA and four

152   autosomal nuclear genes) of population representatives sourced from Mutton et al. (2019).

153   We left a range of specimens unassigned when their source populations were not genetically

154   determined or when they were not genetically determined and were captured at localities near

155   the narrow clades overlap zones. Because of the current lack of clarity around whether the

156   genetic lineages of *A. stuartii* "north" and "south" represent true species, we refer to the three

157   taxonomic units of *A. stuartii* "north", *A. stuartii* "south", and *A. subtropicus* as "clades"

158   throughout this manuscript.

159   We used a GoMeasure 3D HDI109 blue light surface scanner (LMI Technologies Inc.

160   Vancouver, Canada) to create the 3D models. This scanner was portable, allowing us to carry

161   it to museum collections around Australia (Queensland Museum, Australian Museum and

162   Australian National Wildlife Collection). Scanning was undertaken according to protocols

163   developed by Marcy *et al.* (2018) and Viacava *et al.* (2020). We placed each skull specimen

164   in 3 different orientations on a motorised rotary table turning every 45 degrees (8 rotations per

165   round). We meshed together the 24 resulting 3D models with the scanner's software

166   FLEXSCAN3D 3.3 to produce a final 3D model of the complete skull. This 3D model was then

167   cleaned, decimated and reformatted following Viacava *et al.*'s (2020) protocol. Photographs

168   of each specimen helped identify landmarks – for example, we were able to discriminate the

169   nasal-maxillary suture, visible in photographs, from non-biological 3D artefacts.

170   The landmarking template is an adaptation of Viacava *et al.*'s (2020) template based

171   on another dasyurid, the northern quoll (*Dasyurus hallucatus*). This template consists of 412

172   landmarks: 82 fixed landmarks, 63 curves (185 semilandmarks) and 9 surface patches (145

173   semilandmarks) (see landmark locations and their anatomical definitions in Supplementary

174   Figure 5 and Supplementary Table 1, respectively). We avoided landmarking the zygomatic

175   arches because their thin geometry was not captured well at the scanner's resolution.

176   Moreover, the preparation of the skeleton can cause errors on small specimens because

7

177 zygomatic arches can warp after losing support from the muscles during dehydration

178 (Yezerinac, Lougheed, & Handford, 1992; Schmidt *et al.*, 2010). However, the acquisition of

179 a substantial number of specimens and generous coverage of the anatomical zones

180 surrounding the zygomatic arches have been shown to surmount this issue (Marcy *et al.*,

181 2018).

182 All fixed landmarks and curves were manually registered by P. V. in Viewbox version

183 4.0 (dHAL software, Kifissia, Greece). Curve semilandmarks were projected onto the curves,

184 placed equidistantly and were finally slid along their respective curves in Viewbox. Surface

185 semilandmarks followed a thin-plate spline interpolation between the template and each

186 specimen, then were projected to the surface and were finally slid. All sliding procedures were

187 performed following minimization of the bending energy (Bookstein, 1997).

188 **b) *Analyses***

189 We analysed the 3D raw coordinates in R version 3.6.3 (R Core Team, 2019), using the

190 packages "geomorph" (version 3.1.3) (Adams & Otárola- Castillo, 2013), "Morpho" (version

191 2.7) (Schlager *et al.*, 2019) and "landvR" (version 0.5) (Guillerme & Weisbecker, 2019). The

192 first step was to translate, rotate and scale all specimens to the same size by performing a

193 Generalized Procrustes Analysis (GPA). This method results in the decomposition of centroid

194 size and isometry-free shape variation for further analyses (Rohlf & Slice, 1990). Thus, shape,

195 as defined by Kendall (1989), is the resultant of the form of the object minus its isometric

196 component. To analyse shape in each Kendall's morphospace, we performed this GPA step

197 for all specimens and also for the corresponding subsets. For example, when only specimens

198 of known sex or group were considered, the superimposed dataset changed by leaving aside

199 those specimens that were unidentified by sex or group. Note that all analyses involving

200 permutations were set to 1000 iterations, and that Bonferroni adjustments of *p*-values were

201 used to correct for tests involving multiple comparisons .

202 ***Size, allometry and sexual dimorphism***

8

203   We performed pairwise comparisons between the centroid size least squares means

204   of each clade to assess if the skulls of each clade were differently sized. Note that centroid

205   sizes were within the same order of magnitude, such that log-transformation was not deemed

206   necessary.

207   We evaluated the influence of size on shape (allometry – the component of shape that

208   depends on size but is not isometric) in the entire dataset with a Procrustes ANOVA. We then

209   used a Homogeneity of Slopes Test to assess whether the allometric slopes differed between

210   sexes and clades. If this was not the case and they shared a common allometric slope, this

211   would enable us to evaluate allometry-free (i.e. free of shape patterns associated to allometry)

212   shape differences between sexes and clades. The latter step requires additional Procrustes

213   ANOVAs including size as a first and sex or clade as a second predictor variable (Table 1).

214

215   ***Inter- and intra-group shape variation***

216   To explore the patterns of the main shape variation and to assess whether it

217   corresponded to clade boundaries, we conducted a Principal Component Analysis (PCA) on

218   the landmark coordinates. We labelled the groups in the plot of the First and Second Principal

219   Component (PC) scores. We then conducted a Procrustes ANOVA to test whether the groups

220   were morphologically different. We then performed permutation-based pairwise comparisons

221   between mean shapes of these groups.

222   We also performed pairwise comparisons of disparity to evaluate if the clades and

223   sexes differed in morphospace occupancy. Several measurements of disparity are possible

224   (Guillerme *et al.*, 2020), but here we consider the widely-used Procrustes variance. This asks

225   if the residuals of a common linear model fit differ in magnitude between groups, which is

226   possible even if there are no significant differences in shape between groups.

227   Additionally, we aimed to determine the linear distances between landmarks that our

228   analyses suggested to be the most variable between clades. The linear measurements that

9

229   best distinguish the clades were determined by creating heat maps of landmark displacement

230   between the mean shapes of each clade (which is also what is used to determine statistical

231   differences between clades in Procrustes ANOVAs). We colourised landmarks according to

232   how great the displacement is between shapes for each landmark (see the "landvR" package

233   for details) (Guillerme & Weisbecker, 2019). The darkest, most displaced among the

234   landmarks were chosen as candidates for linear measurements to differentiate clades. The

235   goal was to provide a measure of shape differentiation between clades that was easily

236   reproducible in taxonomic museum work. To test for differences between clades, we ran a

237   linear model of these linear distances against centroid size to correct for size, and performed

238   post hoc Tukey multiple comparison tests between means of the clades.

239

240   ***Ecomorphological characterisation***

241   We conducted a variation partitioning analysis of cranial shape for variables that

242   potentially contribute to cranial shape variation. The factors included in the final model were

243   size (as centroid size), the geographic distances among specimens (based on location of

244   capture) and four environmental variables (temperature, temperature seasonality,

245   precipitation and precipitation seasonality). Elevation was initially included as a geographic

246   factor but did not have a clear effect on shape variation and was therefore not retained in the

247   final model. We avoided spatial autocorrelation by transforming the latitude and longitude

248   coordinates of each individual into a principal coordinates neighbourhood matrix (Borcard &

249   Legendre, 2002) and retaining only the axes with positive eigenvalues. We tested for

250   significance in shape variation of the selected axes and included those that were significant in

251   the final variation partitioning model of shape variation. We obtained the environmental

252   variables from the Atlas of Living Australia (www.ala.org.au) and WORLDCLIM (v 2.0)

253   (www.worldclim.org/bioclim) (O'Donnell & Ignizio, 2012). Temperature seasonality (BIO4) is

254   calculated as the standard deviation of the monthly mean temperatures to the mean monthly

255   temperature. Precipitation seasonality (BIO15) is calculated as the ratio of the standard

256   deviation of the monthly total precipitation to the mean monthly total precipitation. Both

257   seasonality variables are known as coefficients of variation and are expressed as a

258   percentage. To partition the shape variation with respect to these environmental variables, we

259   used the *varpart* function in the "vegan" package for R version 3.6.3 (Oksanen *et al.*, 2018).

260   We complemented this analysis with a redundancy analysis ordination on partial and full

261   models (1000 permutations). Finally, to discern how each environmental variable influences

262   shape, we performed a separate variation partitioning analysis of cranial shape with only the

263   four environmental variables.

264   **III.   Results**

265   ***Allometry and sexual dimorphism***

266   The statistics for all the following results are shown in Table 1. In the entire dataset,

267   Procrustes ANOVA revealed that size accounted for 13.3 % of the shape variation ($R^2 = 0.133$;

268    $p = 0.001$). Males were significantly larger than females (also see boxplots in Supplementary

269   Figure 1). Without allometric correction, we found small shape differences between sexes.

270   However, both sexes followed the same allometric slope, allowing us to test if the sexual shape

271   differences were only due to the differential size between sexes. After accounting for size, no

11

272 **Table 1:** ANOVA on predictors of size variation and Procrustes ANOVA on predictors of shape variation.

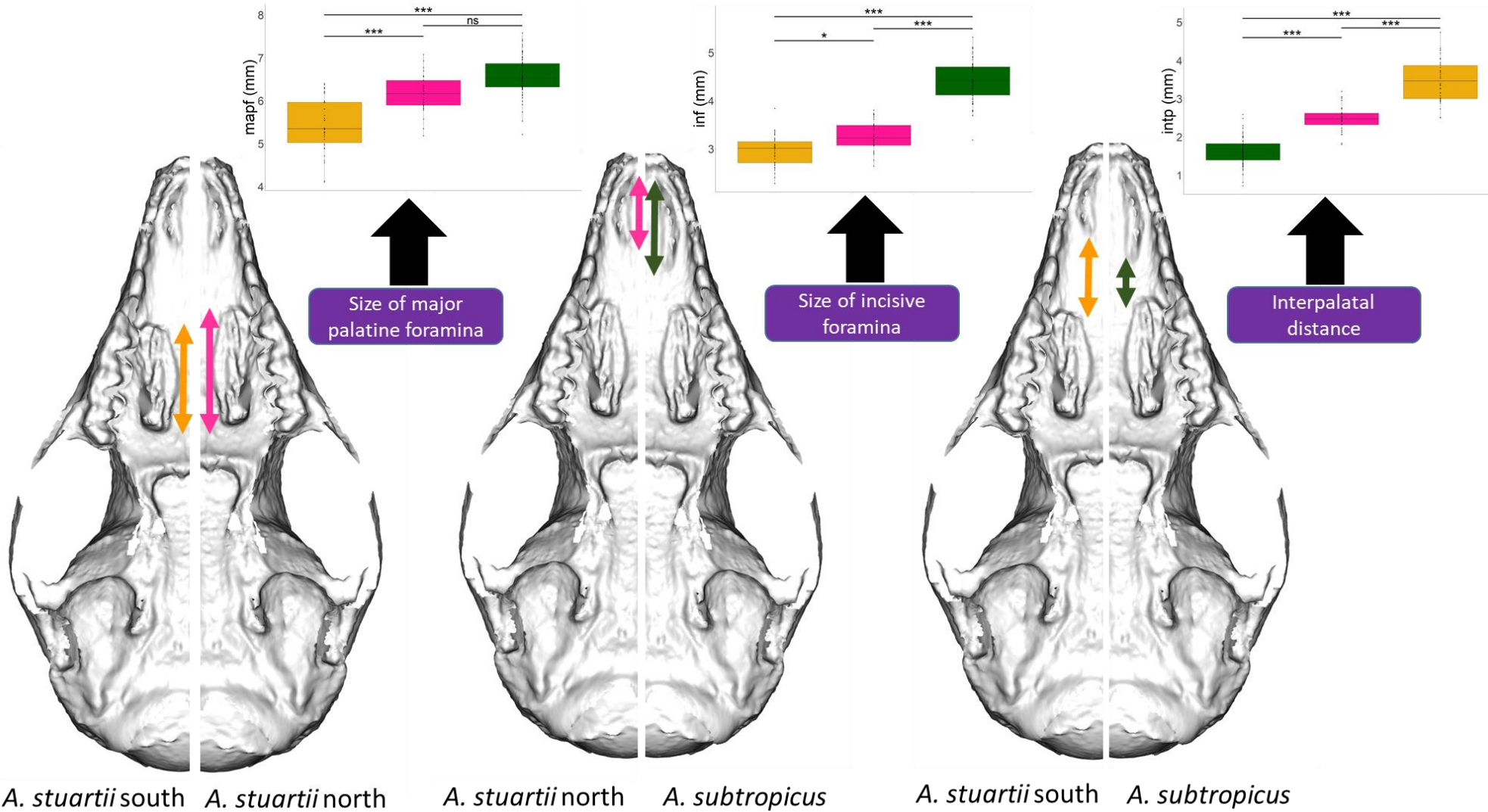| RESPONSE VARIABLE	PREDICTOR VARIABLE	QUESTION	D. F.	SS	R²	F	Pr(>F)	INTERPRETATION
Size	Clade	Are clades different in size?	2	5104.8	0.338	33.925	0.001	Clear effect.
	Sex	Are sexes different in size?	1	5184.7	0.352	71.46	< 0.001	Clear effect.
Shape	Clade	Are clades different in shape?	2	0.017	0.143	11.082	0.001	Clear effect.
	Size	Is there allometry?	1	0.016	0.133	20.477	0.001	Clear effect.
	Sex	Are sexes different in shape?	1	0.004	0.038	5.051	0.001	Low effect sizes and low variance explained.
	Size : Sex	As there is sexual dimorphism and allometry, do sexes differ in allometric slopes?	1	0.001	0.006	0.907	0.587	No clear effect.
	Size + Sex	Adjusting for size, are sexes different in shape?	1	0.001	0.013	1.946	0.016	Low effect sizes and low variance explained.
	Size : Clade	Do clades differ in allometric slopes?	2	0.001	0.012	1.014	0.433	No clear effect.
	Size + Clade	Adjusting for size, are clades different in shape?	2	0.01	0.085	7.175	0.001	Clear effect.

273

274   clear differences were found between sexes. Thus, size differences between males and

275   females almost entirely account for the shape differences between sexes.

276   Centroid size differences were clear only between the larger *A. subtropicus* and the

277   smaller *A. stuartii* (see also boxplots in Figure 2). Before allometric correction, 14.3% of shape

278   variation of the sample was associated with shape differentiation between clades. As with

279   sexes, the clades followed a common allometric slope allowing us to test if the shape

280   differences between clades were purely due to allometry. Unlike the sex comparisons, this

281   was not the case: allometry-free shape differences between clades were significant and

282   accounted for 8.5% of the shape variation.
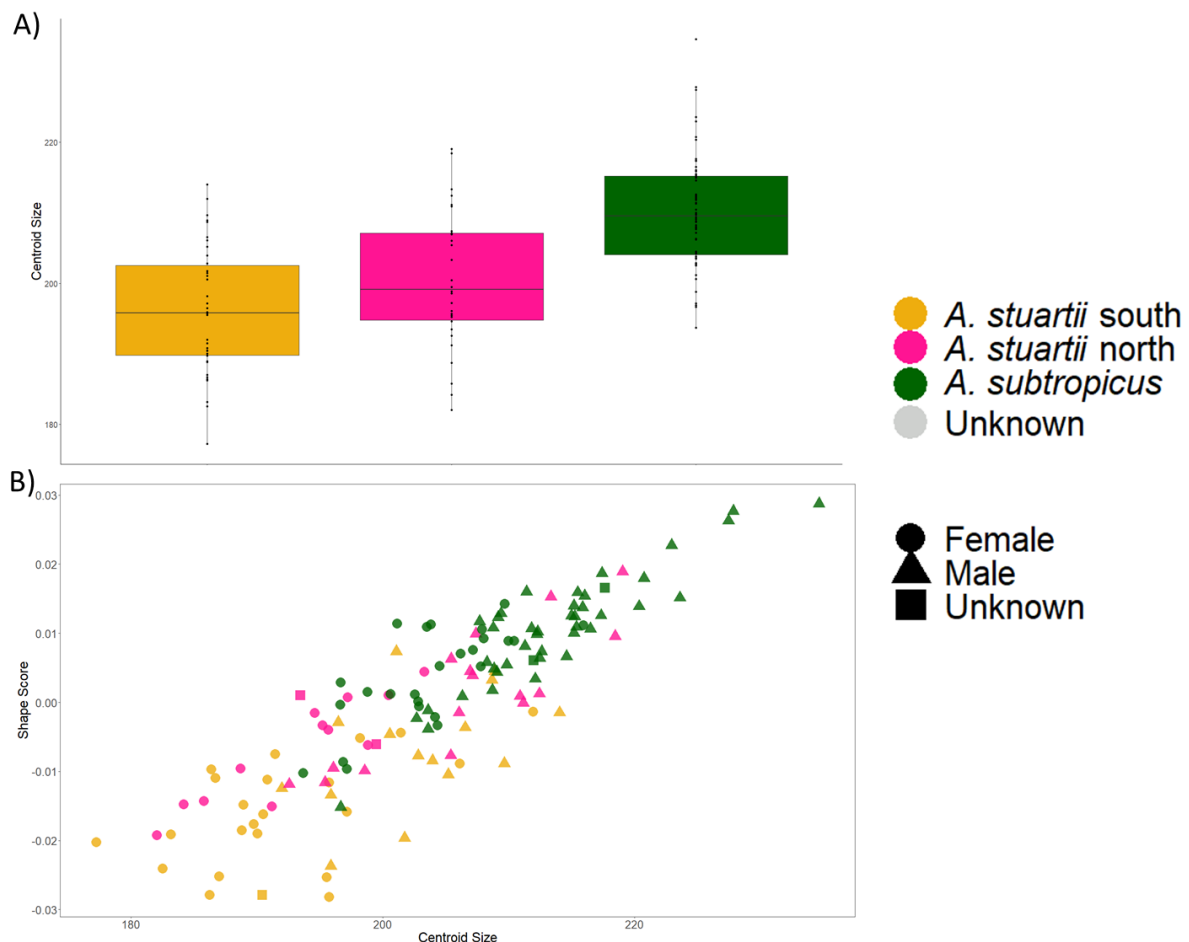
283

284   **Figure 2:** A) Box plot and dot plot of centroid size labelling each clade as per Figure 1.
285   Centroid size differences were clear only between the *larger A. subtropicus* and the smaller
286   *A. stuartii* (both mean comparisons between *A. subtropicus* and the two clades of *A. stuartii*
287   were significant; p = 0.003), but not between *A. stuartii* south and *A. stuartii* north (p = 0.282).
288   B) Allometry plot consisting of centroid sizes versus shape scores obtained from the
289   regression of shape on size (Drake & Klingenberg, 2008).

13

A. stuartii south   A. stuartii north   A. stuartii north   A. subtropicus   A. stuartii south   A. subtropicus

Size of major palatine foramina

Size of incisive foramina

Interpalatal distance

293 **Figure 3:** Pairwise comparisons between mean shapes of each clade (*A. stuartii* south vs *A.*
294 *stuartii* north, p = 0.003; *A. stuartii* north vs *A. subtropicus*, p = 0.003; *A. stuartii* south vs *A.*
295 *subtropicus*, p = 0.003; all p-values were adjusted with following the Bonferroni method). The
296 3D images are the specimen closest to the overall mean warped correspondingly to the mean
297 shapes of each clade. Tukey post-hoc analyses of linear measurements after size correction
298 were performed; significance levels (*p<0.05, **p<0.01, ***p<0.001) are shown in the boxplots.
299 For each comparison, we label the best differentiator diagnostic; i.e., the size of the major
300 palatine foramina (mapf) for differentiating *A. stuartii* south and *A. stuartii* north, the size of the
301 incisive foramina (inf) for differentiating *A. stuartii* north and *A. subtropicus*, and the interpalatal
302 distance (intp) for differentiating between the three clades. Clades are consistently labelled as
303 per Figure 1.

304

305   ***Inter- and intra-group shape variation***

306 The first two principal components represented 28.23 % of the total shape variation (PC1 =

307 19.68%; PC2 = 8.55%) (Supplementary Figure 2). We found clear shape differences between

308 clades (R^2 = 0.143; $F_{1, 127}$ = 11.082; p = 0.001). Pairwise comparisons showed that the three

309 clades clearly differed in shape from each other (all three pairwise comparisons between

310 means: p = 0.001) (also see Figure 3). *Antechinus subtropicus* had larger major palatine

311 foramina and larger incisive foramina, thus with a smaller interpalatal distance compared to

312 both *A. stuartii* lineages. *Antechinus stuartii* north had larger major palatine foramina than *A.*

313 *stuartii* south and smaller incisive foramina than *A. subtropicus* (similar to *A. stuartii* south).

314 *Antechinus stuartii* south had smaller major palatine foramina than *A. stuartii* north and *A.*

315 *subtropicus*. We also observed a slight difference of molar row length, larger in *A. stuartii* south

316 when compared to *A. stuartii* north and *A. subtropicus*. We found no clear morphological

317 disparity (Procrustes variance) differences between lineages (*A. stuartii* south vs *A. stuartii*

318 *north*, p = 0.712; *A. stuartii* north vs *A. subtropicus*, p = 0.93; *A. stuartii* south vs *A. subtropicus*,

319 p = 0.734).

320 Heat maps of landmark displacements between clade mean shapes revealed a striking

321 dominance of just a few landmarks differentiating them. These were the most anterior point of

322 the major palatine foramen and the most posterior point of the incisive foramen

323 (Supplementary Figure 3). We therefore deemed the most distinguishable character between

324 the three lineages to be the distance between the major palatine and incisive foramen (the

325   interpalatal distance – Fig. 3). We measured this distance, averaged both sides for each

326   specimen and determined the distance ranges between these two landmarks for each lineage

327   (Figure 3). All three lineages were clearly different in this character between each other (p <

328   0.001). Post hoc Tukey's multiple comparisons between clade means of three linear distances

329   involving the most variable landmarks revealed linear measurements with potential for

330   distinguishing clades (see boxplots of Figure 3). The size of the major palatine foramina

331   differentiated *A. stuartii* south vs *A. stuartii* north (p < 0.001) and *A. stuartii* south vs *A.*

332   *subtropicus* (p < 0.001) but did not differentiate *A. stuartii* north vs *A. subtropicus* (p = 0.678).

333   The size of the incisive foramina differentiated *A. stuartii* south vs *A. subtropicus* (p < 0.001),

334   *A. stuartii* north vs *A. subtropicus* (p < 0.001) and *A. stuartii* south vs *A. stuartii* north (p =

335   0.0228). The interpalatal distance differentiated *A. stuartii* south vs *A. subtropicus* (p < 0.001),

336   *A. stuartii* north vs *A. subtropicus* (p < 0.001) and *A. stuartii* south vs *A. stuartii* north (p <

337   0.001).

338   ***Ecomorphological characterization***

339   The geographic effect on shape was significant in the *A. stuartii - A. subtropicus* species

340   complex (refer to Table 2 for significance levels and effect sizes). Latitude and longitude were

341   significantly contributing factors to both shape and size variation (see Table 2). However, the

342   geographic variation is confounded with the geographic distribution of clades along the east

343   coast: within-clade geographic analyses did not show clear effects latitudinally nor

344   longitudinally on size and shape (Table 2). Only members of *A. stuartii* south showed

345   significant geographic variation (latitude and longitude) in shape, but they were weakly related

346   (Table 2).

347   We partitioned the contribution of geography, size and climate (precipitation + precipitation

348   seasonality + temperature + temperature seasonality) to the varpart model (Figure 4). The full

16

349 **Table 2:** Analyses of Variance on geographic sources of size and shape variation of the entire A. stuartii - A. subtropicus species complex and
350 within each clade.

| RESPONSE VARIABLE	PREDICTOR VARIABLE	QUESTION	SS	R^2	F	Pr (>F)	INTERPRETATION
Size	Latitude	Is latitude covarying with size in this dataset?	3735.5	0.195	40.29	0.001	Clear effect.
	Latitude within each clade	Is latitude covarying with size within each clade?	South: 104.32 North: 303.04 Sub: 4.7	South: 0.035 North: 0.111 Sub: 0.001	South: 1.311 North: 1.08 Sub: 0.073	South: 0.261 North: 0.061 Sub: 0.813	No clear effect.
	Longitude	Is longitude covarying with size in this dataset?	3428.9	0.179	36.261	0.001	Clear effect.
	Longitude within each clade	Is longitude covarying with size within each clade?	South: 21.16 North: 485.53 Sub: 31	South: 0.007 North: 0.178 Sub: 0.007	South: 0.258 North: 6.07 Sub: 0.478	South: 0.629 North: 0.027 Sub: 0.461	No clear effect. North might have a biased sample.
Shape	Latitude	Is latitude covarying with shape in this dataset?	0.014	0.093	17.054	0.001	Clear effect
	Latitude within each clade	Is latitude covarying with shape within each clade?	South: 0.002 North: 0.001 Sub: 0.001	South: 0.07 North: 0.052 Sub: 0.025	South: 2.705 North: 1.543 Sub: 1.667	South: 0.001 North: 0.058 Sub: 0.039	Only south stuartii is varying latitudinally in shape with low effect.
	Longitude	Is longitude covarying with shape in this dataset?	0.012	0.081	14.645	0.001	Clear effect
	Longitude within each clade	Is longitude covarying with shape within each clade?	South: 0.002 North: 0.001 Sub: 0.001	South: 0.066 North: 0.051 Sub: 0.022	South: 2.554 North: 1.494 Sub: 1.461	South: 0.003 North: 0.09 Sub: 0.117	Only south stuartii is varying longitudinally in shape with low effect.

351

352 **Table 3:** ANOVA on climatic predictors of size variation and Procrustes ANOVA on climatic predictors of shape variation.

	d. f.	Size				Shape			
		SS	R²	F	Pr(>F)	SS	R²	F	Pr(>F)
Precipitation	1	731	0.032	6.596	0.011	0.002	0.013	2.135	0.012
Precipitation seasonality	1	3193.6	0.162	33.27	<0.001	0.012	0.08	14.521	0.001
Temperature	1	4550.7	0.233	51.83	<0.001	0.011	0.075	13.5	0.001
Temperature seasonality	1	1906.7	0.094	18.38	<0.001	0.002	0.016	2.69	0.004
Elevation	1	390.2	0.015	3.457	0.065	0.001	0.006	1.048	0.382

353

354   model showed a significant effect on shape variation ($F_{15,152}$ = 3.981, adjusted R^2 = 0.211, p =

355   0.001). Pure geographic distances contributed 3% on shape variation ($F_{10,152}$ = 1.593, adjusted

356   R^2 = 0.029, p = 0.001). Size alone explained 8% of the variance in the varpart model ($F_{1,152}$ =

357   17.025, adjusted R^2 = 0.083, p = 0.001). Climatic variables alone only contributed to less than

358   1% of the variance ($F_{4,152}$ = 1.375, adjusted R^2 = 0.008); however, when considered jointly

359   with geography, climate and geography explained 9% of the shape variation in the model

360   ($F_{4,163}$ = 5.211, adjusted R^2 = 0.092, p = 0.001). Of the four environmental variables considered

361   in the model, precipitation seasonality and temperature jointly contributed the most to shape

362   variation (Figure 4 and Table 3).
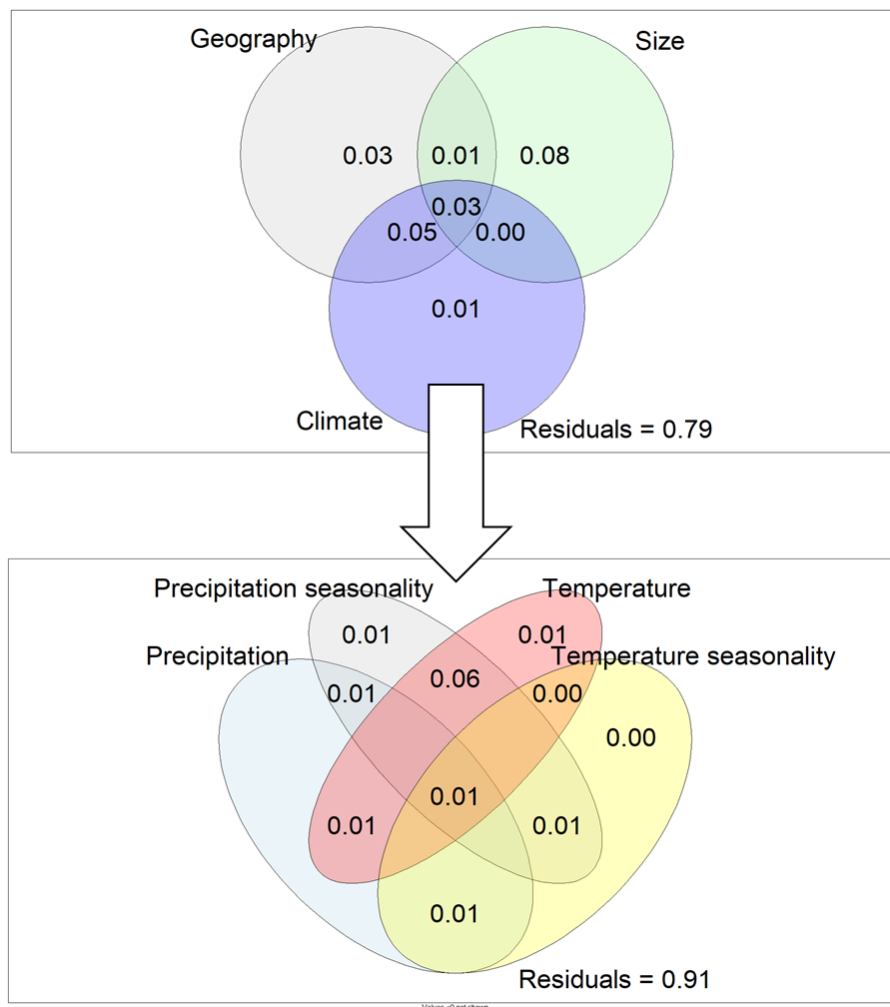
363

364   **Figure 4:** Venn diagrams illustrating variation partitioning analyses. Each individual fraction
365   for each factor contributing to the model is shown in every set. Circle sizes and white space
366   out of the circles representing the unexplained variation are schematic and not to scale.

19

IV. Discussion

Antechinus species have undergone multiple taxonomic revisions, with recent genetic data suggesting substantially higher biodiversity within the genus than previously expected. Here, we corroborated the genetic differences between *A. stuartii* north and *A. stuartii* south observing clear morphological differences in the major palatine foramina. Thus, we have provided a cranial morphological differentiator in support of Mutton et al.'s (2019) suggestion that *A. stuartii* south and *A. stuartii* north should be reclassified as separate species, within the scope of the phylogenetic species concept (Nixon & Wheeler, 1990). We also corroborated shape differences between *A. subtropicus* and *A. stuartii* and provided an easy-to-follow morphological differentiation protocol for skulls of the three lineages. Additionally, among the environmental variables considered, precipitation seasonality and temperature were the most important factors for shaping the skull in the *A. stuartii - A. subtropicus* complex. This renders the species group of particular conservation concern because it is located on the east coast of Australia, a zone increasingly impacted by climate change (Di Virgilio *et al.*, 2019; Dowdy *et al.*, 2019; Kirono *et al.*, 2020), which is expected to cause variation in precipitation seasonality, temperature and fire weather. Importantly, the distributional ranges of *A. stuartii* south and *A. stuartii* north fall directly within the burn zone of 2019-2020 mega-fires, and the results of the present study add support to a case for the separate management of these taxa.

Differences in palatal vacuity size and molar row length, which we found as important differentiators in our investigation, are widely recognized as diagnostically useful for species identification in various marsupials. For example, the size of the palatal vacuities differentiate species of potoroids, e.g., *Bettongia* (McDowell *et al.*, 2015) and peramelids, e.g., *Microperoryctes* (Groves & Flannery, 1990). Dasyurid species have also been diagnosed in consideration of palatal vacuity size, e.g., *Sminthopsis* (Archer, 1981; Kemper *et al.*, 2011); and more specifically, several species of *Antechinus* (Van Dyck, 1982; Dickman *et al.*, 1998; Baker *et al.*, 2012, 2014). We also add a new differentiating skull trait of molar row length for the clades studied here, which is possibly linked to allometry. This taxonomic differentiator has

20

394   been found for other antechinus species varying in absolute size (Baker *et al.*, 2012, 2013;

395   Baker & Van Dyck, 2013b). Molar row length has also been found to separate diverse

396   mammals such as rodents (Anderson & Yates, 2000; Christoff *et al.*, 2000; Gonçalves,

397   Almeida, & Bonvicino, 2005; Boroni *et al.*, 2017), shrews (Balčiauskienė, Juškaitis, &

398   Mažeikytė, 2002), bats (Bogdanowicz, 1990), wombats (Black, 2007) and didelphids (Voss,

399   Lunde, & Jansa, 2005).

400   Our geographic analyses suggest that the latitudinal shape variation observed across

401   the entire dataset is likely driven by morphological differences between the taxa; however, this

402   latitudinal shape variation is not strongly associated with shape within each taxon (see Table

403   2). This suggests that clinal variation does co-vary with the shape differentiation between the

404   three clades and the clinal variation we observe in the whole dataset is a result of, but not

405   notably influenced by, the clinal distribution of the three taxa. This appearance of a clinal effect

406   would be even stronger under the old taxonomic combination of *A. stuartii* south and north as

407   one species (rather than *A. stuartii* north being sister taxa of *A. subtropicus*), which may have

408   prompted previous suggestions that the variation between species of *Antechinus* may be

409   driven clinally (Van Dyck & Crowther, 2000) (i.e., climatically/geographically). However, the

410   nature of the variation within the genus and its relation to latitude should be investigated in a

411   broader sample of antechinus species, particularly since there have been suggestions that *A.*

412   *subtropicus* is more similar morphologically to the less genetically closely related *A. agilis* than

413   it is to *A. stuartii* (Dickman *et al.*, 1998; Van Dyck & Crowther, 2000; Crowther, 2002; Crowther,

414   Sumner, & Dickman, 2003). Regardless, finding little or no clinal shape variation *within* each

415   clade (also suggested for the whole of *A. stuartii* by (Crowther *et al.*, 2003)) suggests that

416   speciation-related differences in morphology are independent of within-species variation in

417   these antechinus taxa (a pattern also found in wombats (Weisbecker *et al.*, 2019)).

418   Our results add some insights on the putative processes behind the speciation event

419   in the young clades of the *A. stuartii – A. subtropicus* complex. In 1981, Archer argued that

420   the species of *Sminthopsis* located in inland arid areas had larger palatal vacuities and linked

21

421 the size of the vacuities to aridity. We also found differences in vacuity sizes with smaller major

422 palatine foramina in the southern clade of *A. stuartii* relative to the northern clade and *A.*

423 *subtropicus*. Although we did not find a strong influence of precipitation or aridity with shape

424 variation in this species complex, shape variation was strongly associated with temperature

425 and precipitation seasonality variation. In particular, rainfall seasonality is associated with food

426 abundance predictability (Kishimoto- Yamada & Itioka, 2015), which appears tied to variation

427 in breeding times observed in antechinus species and is hypothesized to have driven the

428 evolution of semelparity in these dasyurids (Fisher *et al.*, 2013). This environmental factor may

429 have also influenced reproductive isolation involving morphological differentiation. Intriguingly,

430 the shape changes associated with precipitation seasonality involve differences in the size of

431 the palatal vacuities with *A. subtropicus* displaying larger incisive and major palatine foramina

432 than *A. stuartii*. These vacuities convey access to the vomeronasal organ that plays a major

433 role in antechinus reproduction (Aland, Gosden, & Bradley, 2016).

434 The difference in molar row length between *A. stuartii* south relative to *A. stuartii* north

435 is noteworthy because it is reminiscent of a well-known effect where carnassial tooth length

436 differentiates carnivoran species living in sympatry. Garcia-Navas et al. (2020) suggested that,

437 due to the mostly insectivorous nature and lack of carnassial teeth in dasyurids, such an effect

438 is not expected; however, the molar row of dasyurids has in the past been argued to act as a

439 single contiguous shearing blade (Werdelin, 1986, 1987; Smits & Evans, 2012). It is therefore

440 possible that the difference in molar row length we observe is related to an effect of dietary

441 niche partitioning, similar to carnivorans. However, because the molar row length differences

442 are tied to allometry, it is also possible that this pattern is influenced by a more general effect

443 of allometric scaling, such as the distinction of molar row length observed between differently

444 sized *A. argentus*, *A. flavipes* and *A. mysticus* (Baker *et al.*, 2012, 2013; Baker & Van Dyck,

445 2013b).

446 Not all of our findings based on geometric morphometrics are consistent with previous

447 morphological observations based on the analysis of skull proportions. For example, the

22

448 differentiation of *A. stuartii* south with *A. subtropicus* according to molar row length was not

449 observed by Van Dyck & Crowther (2000). Intriguingly also, we did not observe a previously

450 suggested morphological distinction – a longer and narrower rostrum – between *A.*

451 *subtropicus* and *A. stuartii* (Van Dyck & Crowther, 2000). It is possible that the latter

452 discrepancy is mainly due to pure size differences (i.e., non-shape differences) between these

453 two clades, which may be reflected differently in the different analytical approaches.

454 Specifically, the moderate size-related (allometric) shape changes we observe with geometric

455 morphometrics might not be regarded as allometric in linear measurement studies. Traditional

456 morphometric studies focus on maximal lengths and widths, and use ratios as a descriptor for

457 shape. By comparison, in geometric morphometrics, the descriptor of shape includes the

458 relative positions and distances of all landmarks, and size is removed from the equation after

459 Procrustes superimposition. This can cause two types of discrepancy in the analysis of relative

460 size: first, when allometry is analysed in traditional methods, it generally relies on non-scaled

461 or log-scaled measures, whereas when allometry is analysed in geometric morphometrics, the

462 factors taken into account are the calculated centroid size and a scaled abstract shape

463 (Mitteroecker & Gunz, 2009). Thus, it is possible that rostral length measurements may be

464 heavily influenced by differences in size between species, rendering the diagnostic less

465 suitable for differentiating similarly sized individuals of these clades. A potential second issue

466 is that geometric morphometric landmarking protocols of the mammalian cranium generally

467 rely on homologous points such as suture intersections (type I landmarks), rather than

468 frequently employed taxonomic measures of maximum and minimum widths or lengths. Such

469 "extreme points" of shape may therefore be less emphasised by the landmarking protocol. In

470 such cases, the chief consideration should be whether the location of extreme-point

471 measurements relative to the skull may matter.

472   In this study, we have demonstrated the versatility of geometric morphometric

473 research, providing taxonomic discernment in otherwise morphologically cryptic species and

474 inferring biological processes by identifying associations between morphological

475 differentiation, and geographic and environmental factors. On the taxonomic aspect, the

476 resolution of these small cryptic taxa by 3D shape analyses highlights the importance of the

477 method in systematic studies. In the future, these mammal taxa may see their geographic

478 ranges reduced by an elevation to species rank and, unfortunately, their populations diminish

479 due to a fatal coincidence with fire line zones along Eastern Australia.

480

481 **V.   ACKNOWLEDGEMENTS**

491 **VI.   AUTHOR CONTRIBUTIONS:** P. V. and V. W. conceived the ideas; P. V. collected the

492   data; P. V. and V. W. analysed the data with input from A. M. B., S. P. B. and M. J. P.;

493   and P. V. and V. W. led the writing with input from A. M. B., S. P. B. and M. J. P.

494

495 **VII.   DATA AVAILABILITY STATEMENT**

496 Data and R code are publicly available in GitHub. 3D models can also be publicly accessed

497 through Morphosource.

498

499 **VIII.   CONFLICT OF INTEREST**

24

500   The authors declare no conflict of interest.

501

502   **IX.   <u>References</u>**

503   Adams DC, Otárola-Castillo E. 2013. geomorph: an R package for the collection and

504   analysis of geometric morphometric shape data. *Methods in Ecology and Evolution* 4: 393–

505   399.

506   Adams DC, Rohlf FJ, Slice DE. 2013. A field comes of age: geometric morphometrics in the

507   21st century. *Hystrix, the Italian Journal of Mammalogy* 24.

508   Aland RC, Gosden E, Bradley AJ. 2016. Seasonal morphometry of the vomeronasal organ in

509   the marsupial mouse, *Antechinus subtropicus*. *Journal of Morphology* 277: 1517–1530.

510   Anderson S, Yates TL. 2000. A New Genus and Species of Phyllotine Rodent from Bolivia.

511   *Journal of Mammalogy* 81: 18–36.

512   Archer M. 1981. Systematic revision of the marsupial dasyurid genus *Sminthopsis* Thomas.

513   Bulletin of the AMNH ; v. 168, article 2: 65-217.

514   Baker AM, Dickman C. 2018. *Secret lives of carnivorous marsupials*. CSIRO PUBLISHING,

515   Clayton, Victoria.

516   Baker AM, Mutton TY, Hines H. 2013. A new dasyurid marsupial from Kroombit Tops, south-

517   east Queensland, Australia: the Silver-headed antechinus, *Antechinus argentus sp. nov.*

518   (Marsupialia: Dasyuridae). *Zootaxa* 3746: 201–239.

519   Baker AM, Mutton TY, Hines H, Van Dyck S. 2014. The Black-tailed antechinus, *Antechinus*

520   *arktos sp. nov.*: a new species of carnivorous marsupial from montane regions of the Tweed

521   Volcano caldera, eastern Australia. *Zootaxa* 3765: 101–33.

522   Baker AM, Mutton TY, Mason E, Gray EL. 2015. A taxonomic assessment of the Australian

523   dusky antechinus complex: a new species, the Tasman Peninsula dusky antechinus

524   (*Antechinus vandycki* sp. nov.) and an elevation to species of the mainland dusky

525   antechinus (*Antechinus swainsonii mimetes* (Thomas)). *Memoirs of the Queensland*

526   *Museum–Nature* 59: 75–126.

527   Baker AM, Mutton TY, Van Dyck S. 2012. A new dasyurid marsupial from eastern

528   Queensland, Australia: the Buff-footed antechinus, *Antechinus mysticus sp. nov.*

529   (Marsupialia: Dasyuridae). *Zootaxa* 3515: 1–37.

530   Baker AM, Van Dyck S. 2013a. Taxonomy and redescription of the Fawn antechinus,

531   *Antechinus bellus* (Thomas) (Marsupialia: Dasyuridae). *Zootaxa* 3613: 201–228.

532   Baker AM, Van Dyck S. 2013b. Taxonomy and redescription of the Yellow-footed antechinus

533   , *Antechinus flavipes* (Waterhouse) (Marsupialia: Dasyuridae). *Zootaxa* 3649: 1–62.

534   Baker AM, Van Dyck S. 2013c. Taxonomy and redescription of the Atherton Antechinus,

535   *Antechinus godmani* (Thomas) (Marsupialia: Dasyuridae). *Zootaxa* 3670: 401–439.

536   Baker AM, Van Dyck S. 2015. Taxonomy and redescription of the swamp antechinus,

537   *Antechinus minimus* (E. Geoffroy) (Marsupialia: Dasyuridae). *Memoirs of the Queensland*

538   *Museum - Nature* 59: 127–170.

539   Balčiauskienė L, Juškaitis R, Mažeikytė R. 2002. Identification of Shrews and Rodents from

540   Skull Remains according to the Length of a Tooth Row. *Acta Zoologica Lituanica* 12: 353–

541   361.

542   Bickford D, Lohman DJ, Sodhi NS, Ng PKL, Meier R, Winker K, Ingram KK, Das I. 2007.

543   Cryptic species as a window on diversity and conservation. *Trends in Ecology & Evolution*

544   22: 148–155.

545   Black K. 2007. Maradidae: a new family of vombatomorphian marsupial from the late

546   Oligocene of Riversleigh, northwestern Queensland. *Alcheringa: An Australasian Journal of*

547   *Palaeontology* 31: 17–32.

548   Bogdanowicz W. 1990. Geographic Variation and Taxonomy of Daubenton's Bat, *Myotis*

549   *daubentoni* in Europe. *Journal of Mammalogy* 71: 205–218.

550   Bookstein FL. 1997. Landmark methods for forms without landmarks: morphometrics of

551   group differences in outline shape. *Medical Image Analysis* 1: 225–243.

552   Borcard D, Legendre P. 2002. All-scale spatial analysis of ecological data by means of

553   principal coordinates of neighbour matrices. *Ecological Modelling* 153: 51–68.

554   Boroni NL, Lobo LS, Romano PSR, Lessa G, Boroni NL, Lobo LS, Romano PSR, Lessa G.

555   2017. Taxonomic identification using geometric morphometric approach and limited data: an

556   example using the upper molars of two sympatric species of *Calomys* (Cricetidae: Rodentia).

557   *Zoologia (Curitiba)* 34.

558   Bowman DMJS, Kolden CA, Abatzoglou JT, Johnston FH, van der Werf GR, Flannigan M.

559   2020. Vegetation fires in the Anthropocene. *Nature Reviews Earth & Environment* 1: 500–

560   515.

561   Bryant LM, Fuller SJ. 2014. Pleistocene climate fluctuations influence phylogeographical

562   patterns in *Melomys cervinipes* across the mesic forests of eastern Australia. *Journal of*

563   *Biogeography* 41: 1923–1935.

564   Bryant LM, Krosch MN. 2016. Lines in the land: a review of evidence for eastern Australia's

565   major biogeographical barriers to closed forest taxa. *Biological Journal of the Linnean*

566   *Society* 119: 238–264.

567   Chaplin K, Sumner J, Hipsley CA, Melville J. 2020. An Integrative Approach Using

568   Phylogenomics and High-Resolution X-Ray Computed Tomography for Species Delimitation

569   in Cryptic Taxa. *Systematic Biology* 69: 294–307.

570   Chapple DG, Chapple SNJ, Thompson MB. 2011a. Biogeographic barriers in south-eastern

571   Australia drive phylogeographic divergence in the garden skink, *Lampropholis guichenoti*.

572   *Journal of Biogeography* 38: 1761–1775.

573   Chapple DG, Hoskin CJ, Chapple SN, Thompson MB. 2011b. Phylogeographic divergence

574   in the widespread delicate skink (*Lampropholis delicata*) corresponds to dry habitat barriers

575   in eastern Australia. *BMC Evolutionary Biology* 11: 191.

576   Christoff AU, Fagundes V, Sbalqueiro IJ, Mattevi MS, Yonenaga-Yassuda Y. 2000.

577   Description of a New Species of *Akodon* (Rodentia: Sigmodontinae) from Southern Brazil.

578   *Journal of Mammalogy* 81: 838–851.

579   Colgan DJ, O'Meally D, Sadlier RA. 2010. Phylogeographic patterns in reptiles on the New

580   England Tablelands at the south-western boundary of the McPherson Macleay Overlap.

581   *Australian Journal of Zoology* 57: 317–328.

582   Crandall KA, Bininda-Emonds ORP, Mace GM, Wayne RK. 2000. Considering evolutionary

583   processes in conservation biology. *Trends in Ecology & Evolution* 15: 290–295.

584   Crowther MS. 2002. Morphological variation within *Antechinus agilis* and *Antechinus stuartii*

585   (Marsupialia : Dasyuridae). *Australian Journal of Zoology* 50: 339–356.

586   Crowther MS, Sumner J, Dickman CR. 2003. Speciation of *Antechinus stuartii* and *A.*

587   *subtropicus* (Marsupialia : Dasyuridae) in eastern Australia: molecular and morphological

588   evidence. *Australian Journal of Zoology* 51: 443.

28

589   Crowther MS, Tulloch AI, Letnic M, Greenville AC, Dickman CR. 2018. Interactions between

590   wildfire and drought drive population responses of mammals in coastal woodlands. *Journal*

591   *of Mammalogy* 99: 416–427.

592   Di Virgilio G, Evans JP, Blake SAP, Armstrong M, Dowdy AJ, Sharples J, McRae R. 2019.

593   Climate Change Increases the Potential for Extreme Wildfires. *Geophysical Research*

594   *Letters* 46: 8517–8526.

595   Dickman CR, Parnaby HE, Crowther MS, King DH. 1998. *Antechinus agilis* (Marsupialia :

596   Dasyuridae), a new species from the A. stuartii complex in south-eastern Australia.

597   *Australian Journal of Zoology* 46: 1–26.

598   Dowdy AJ, Ye H, Pepler A, Thatcher M, Osbrough SL, Evans JP, Di Virgilio G, McCarthy N.

599   2019. Future changes in extreme weather and pyroconvection risk factors for Australian

600   wildfires. *Scientific Reports* 9: 10073.

601   Dubois A. 2003. The relationships between taxonomy and conservation biology

602   in the century of extinctions. *Comptes Rendus Biologies* 326: 9–21.

603   Firth RSC, Brook BW, Woinarski JCZ, Fordham DA. 2010. Decline and likely extinction of a

604   northern Australian native rodent, the Brush-tailed Rabbit-rat *Conilurus penicillatus*.

605   *Biological Conservation* 143: 1193–1201.

606   Fisher DO, Dickman CR, Jones ME, Blomberg SP. 2013. Sperm competition drives the

607   evolution of suicidal reproduction in mammals. *Proceedings of the National Academy of*

608   *Sciences* 110: 17910–17914.

609   Frankham GJ, Handasyde KA, Eldridge MDB. 2012. Novel insights into the phylogenetic

610   relationships of the endangered marsupial genus *Potorous*. *Molecular Phylogenetics and*

611   *Evolution* 64: 592–602.

612 Fraser DJ, Bernatchez L. 2001. Adaptive evolutionary conservation: towards a unified

613 concept for defining conservation units. *Molecular Ecology* 10: 2741–2752.

614 García-Navas V, Kear BP, Westerman M. 2020. The geography of speciation in dasyurid

615 marsupials. *Journal of Biogeography* 47: 2042–2053.

616 Geyle HM, Woinarski JCZ, Baker GB, Dickman CR, Dutson G, Fisher DO, Ford H,

617 Holdsworth M, Jones ME, Kutt A, Legge S, Leiper I, Loyn R, Murphy BP, Menkhorst P,

618 Reside AE, Ritchie EG, Roberts FE, Tingley R, Garnett ST. 2018. Quantifying extinction risk

619 and forecasting the number of impending Australian bird and mammal extinctions. *Pacific*

620 *Conservation Biology* 24: 157–167.

621 Goldingay RL. 2000. Small dasyurid marsupials – are they effective pollinators? *Australian*

622 *Journal of Zoology* 48: 597–606.

623 Goldingay RL, Carthew SM, Whelan RJ. 1991. The Importance of Non-Flying Mammals in

624 Pollination. *Oikos* 61: 79–87.

625 Gonçalves PR, Almeida FC, Bonvicino CR. 2005. A new species of *Wiedomys* (Rodentia:

626 Sigmodontinae) from Brazilian Cerrad. *Mammalian Biology* 70: 46–60.

627 Groves CP, Flannery T. 1990. Revision of the families and genera of bandicoots. *Unknown*

628 *Journal*: 1–11.

629 de Guia APO, Saitoh T. 2007. The gap between the concept and definitions in the

630 Evolutionarily Significant Unit: the need to integrate neutral genetic variation and adaptive

631 variation. *Ecological Research* 22: 604–612.

632 Guillerme T, Puttick MN, Marcy AE, Weisbecker V. 2020. Shifting spaces: Which disparity or

633 dissimilarity measurement best summarize occupancy in multidimensional spaces? *Ecology*

634 *and Evolution* 10: 7261–7275.

635   Guillerme T, Weisbecker V. 2019. *landvR: Tools for measuring landmark position variation*.

636   Zenodo.

637   Holleley CE, Dickman CR, Crowther MS, Oldroyd BP. 2006. Size breeds success: multiple

638   paternity, multivariate selection and male semelparity in a small marsupial, *Antechinus*

639   *stuartii. Molecular Ecology* 15: 3439–3448.

640   Jackson S, Groves C. 2015. *Taxonomy of Australian Mammals*. Csiro Publishing.

641   James CH, Moritz C. 2000. Intraspecific phylogeography in the sedge frog *Litoria fallax*

642   (Hylidae) indicates pre-Pleistocene vicariance of an open forest species from eastern

643   Australia. *Molecular Ecology* 9: 349–358.

644   Kemper CM, Cooper SJB, Medlin GC, Adams M, Stemmer D, Saint KM, McDowell MC,

645   Austin JJ. 2011. Cryptic grey-bellied dunnart (*Sminthopsis griseoventer*) discovered in South

646   Australia: genetic, morphological and subfossil analyses show the value of collecting

647   voucher material. *Australian Journal of Zoology* 59: 127.

648   Kendall DG. 1989. A survey of the statistical Theory of shape. *Statistical Science* 4: 87–99.

649   Kirono DGC, Round V, Heady C, Chiew FHS, Osbrough S. 2020. Drought projections for

650   Australia: Updated results and analysis of model simulations. *Weather and Climate*

651   *Extremes* 30: 100280.

652   Kishimoto-Yamada K, Itioka T. 2015. How much have we learned about seasonality in

653   tropical insect abundance since Wolda (1988)? *Entomological Science* 18: 407–419.

654   Kraaijeveld-Smit FJL, Ward SJ, Temple-Smith PD. 2003. Paternity success and the direction

655   of sexual selection in a field population of a semelparous marsupial, *Antechinus agilis*.

656   *Molecular Ecology* 12: 475–484.

657   Lee AK, Cockburn A. 1985. *Evolutionary Ecology of Marsupials*. Cambridge University

658   Press.

659   Legge S, Robinson N, Lindenmayer D, Scheele B, Southwell D, Wintle B. 2018. *Monitoring*

660   *threatened species and ecological communities*. Csiro Publishing.

661   Letnic M, Tamayo B, Dickman CR. 2005. The Responses of Mammals to La Niña (El Niño

662   Southern Oscillation)–Associated Rainfall, Predation, and Wildfire in Central Australia.

663   *Journal of Mammalogy* 86: 689–703.

664   Lucky A. 2011. Molecular phylogeny and biogeography of the spider ants, genus

665   *Leptomyrmex* Mayr (Hymenoptera: Formicidae). *Molecular Phylogenetics and Evolution* 59:

666   281–292.

667   Marcy AE, Fruciano C, Phillips MJ, Mardon K, Weisbecker V. 2018. Low resolution scans

668   can provide a sufficiently accurate, cost- and time-effective alternative to high resolution

669   scans for 3D shape analyses (P Cox, Ed.). *PeerJ* 6: e5032.

670   May RM. 1988. How Many Species Are There on Earth? *Science* 241: 1441–1449.

671   McDowell MC, Haouchar D, Aplin KP, Bunce M, Baynes A, Prideaux GJ. 2015.

672   Morphological and molecular evidence supports specific recognition of the recently extinct

673   *Bettongia anhydra* (Marsupialia: Macropodidae). *Journal of Mammalogy* 96: 287–296.

674   McGuigan K, McDonald K, Parris K, Moritz C. 1998. Mitochondrial DNA diversity and

675   historical biogeography of a wet forest-restricted frog (*Litoria pearsoniana*) from mid-east

676   Australia. *Molecular Ecology* 7: 175–186.

677   Mitteroecker P, Gunz P. 2009. Advances in geometric morphometrics. *Evolutionary Biology*

678   36: 235–247.

679   Murphy BP, Woolley LA, Geyle HM, Legge SM, Palmer R, Dickman CR, Augusteyn J, Brown

680   SC, Comer S, Doherty TS, Eager C, Edwards G, Fordham DA, Harley D, McDonald PJ,

681   McGregor H, Moseby KE, Myers C, Read J, Riley J, Stokeld D, Trewella GJ, Turpin JM,

682   Woinarski JCZ. 2019. Introduced cats (*Felis catus*) eating a continental fauna: The number

683   of mammals killed in Australia. *Biological Conservation* 237: 28–40.

684   Mutton TY, Phillips MJ, Fuller SJ, Bryant LM, Baker AM. 2019. Systematics, biogeography

685   and ancestral state of the Australian marsupial genus *Antechinus* (Dasyuromorphia:

686   Dasyuridae). *Zoological Journal of the Linnean Society* 186: 553–568.

687   Nixon KC, Wheeler QD. 1990. An Amplification of the Phylogenetic Species Concept.

688   *Cladistics* 6: 211–223.

689   O'Donnell MS, Ignizio DA. 2012. Bioclimatic predictors for supporting ecological applications

690   in the conterminous United States. *US Geological Survey Data Series* 691.

691   Oksanen J, Blanchet FG, Friendly M, Kindt R, Legendre P, McGlinn D, Minchin PR, O'Hara

692   RB, Simpson GL, Solymos P. 2018. vegan: Community ecology package. R package

693   version 2.5-2. 2018.

694   Pardon LG, Brook BW, Griffiths AD, Braithwaite RW. 2003. Determinants of survival for the

695   northern brown bandicoot under a landscape-scale fire experiment. *Journal of Animal*

696   *Ecology* 72: 106–115.

697   Pastro L. 2013. The effects of wildfire on small mammals and lizards in The Simpson Desert,

698   Central Australia.

699   R Core Team. 2019. R: A language and environment for statistical computing. R Foundation

700   for Statistical Computing, Vienna, Austria.

701   Radford JQ, Woinarski JCZ, Legge S, Baseler M, Bentley J, Burbidge AA, Bode M, Copley

702   P, Dexter N, Dickman CR, Gillespie G, Hill B, Johnson CN, Kanowski J, Latch P, Letnic M,

703   Manning A, Menkhorst P, Mitchell N, Morris K, Moseby K, Page M, Ringma J. 2018.

704   Degrees of population-level susceptibility of Australian terrestrial non-volant mammal

705   species to predation by the introduced red fox (*Vulpes vulpes*) and feral cat (*Felis catus*).

706   *Wildlife Research* 45: 645–657.

707   Rix MG, Harvey MS. 2012. Phylogeny and historical biogeography of ancient assassin

708   spiders (Araneae: Archaeidae) in the Australian mesic zone: Evidence for Miocene

709   speciation within Tertiary refugia. *Molecular Phylogenetics and Evolution* 62: 375–396.

710   Rohlf FJ, Slice D. 1990. Extensions of the Procrustes method for the optimal superimposition

711   of landmarks. *Systematic Biology* 39: 40–59.

712   Rowe KMC, Rowe KC, Elphinstone MS, Baverstock PR. 2012. Population structure, timing

713   of divergence and contact between lineages in the endangered Hastings River mouse

714   (*Pseudomys oralis*). *Australian Journal of Zoology* 59: 186–200.

715   Schlager S, Jefferis G, Ian D, Schlager MS. 2019. Package 'Morpho'.

716   Schmidt EJ, Parsons TE, Jamniczky HA, Gitelman J, Trpkov C, Boughner JC, Logan CC,

717   Sensen CW, Hallgrímsson B. 2010. Micro-computed tomography-based phenotypic

718   approaches in embryology: procedural artifacts on assessments of embryonic craniofacial

719   growth and development. *BMC Developmental Biology* 10: 18.

720   Smits PD, Evans AR. 2012. Functional constraints on tooth morphology in carnivorous

721   mammals. *BMC Evolutionary Biology* 12: 146.

722   Sumner J, Dickman CR. 1998. Distribution and identity of species in the *Antechinus stuartii* -

723   *A. flavipes* group (Marsupialia : Dasyuridae) in south-eastern Australia. *Australian Journal of*

724   *Zoology* 46: 27.

725   Ukkola AM, Kauwe MGD, Roderick ML, Abramowitz G, Pitman AJ. 2020. Robust Future

726   Changes in Meteorological Drought in CMIP6 Projections Despite Uncertainty in

727   Precipitation. *Geophysical Research Letters* 47: e2020GL087820.

728   Van Dyck S. 1982. The status and relationships of the Atherton antechinus, *Antechinus*

729   *godmani* (Marsupialia: Dasyuridae). *Australian Mammalogy* 5: 195–210.

730   Van Dyck S, Crowther MS. 2000. Reassessment of northern representatives of the

731   *Antechinus stuartii* complex (Marsupialia: Dasyuridae): *A subtropicus sp. nov.* and *A.*

732   *adustus* new status. *MEMOIRS-QUEENSLAND MUSEUM* 45: 611–635.

733   Viacava P, Blomberg SP, Sansalone G, Phillips MJ, Guillerme T, Cameron SF, Wilson RS,

734   Weisbecker V. 2020. Skull shape of a widely distributed, endangered marsupial reveals little

735   evidence of local adaptation between fragmented populations. *Ecology and Evolution* 10:

736   9707–9720.

737   Voss RS, Lunde DP, Jansa SA. 2005. On the Contents of Gracilinanus Gardner and

738   Creighton, 1989, with the Description of a Previously Unrecognized Clade of Small Didelphid

739   Marsupials. *American Museum Novitates* 2005: 1–36.

740   Ward M, Tulloch AIT, Radford JQ, Williams BA, Reside AE, Macdonald SL, Mayfield HJ,

741   Maron M, Possingham HP, Vine SJ, O'Connor JL, Massingham EJ, Greenville AC,

742   Woinarski JCZ, Garnett ST, Lintermans M, Scheele BC, Carwardine J, Nimmo DG,

743   Lindenmayer DB, Kooyman RM, Simmonds JS, Sonter LJ, Watson JEM. 2020. Impact of

744   2019–2020 mega-fires on Australian fauna habitat. *Nature Ecology & Evolution* 4: 1321–

745   1326.

746   Weisbecker V, Guillerme T, Speck C, Sherratt E, Abraha HM, Sharp AC, Terhune CE,

747   Collins S, Johnston S, Panagiotopoulou O. 2019. Individual variation of the masticatory

748   system dominates 3D skull shape in the herbivory-adapted marsupial wombats. *Frontiers in*

749   *Zoology* 16: 41.

750   Werdelin L. 1986. Comparison of skull shape in marsupial and placental carnivores.

751   *Australian Journal of Zoology* 34: 109–117.

752   Werdelin L. 1987. Jaw Geometry and Molar Morphology in Marsupial Carnivores: Analysis of

753   a Constraint and Its Macroevolutionary Consequences. *Paleobiology* 13: 342–350.

754   Woinarski JCZ, Burbidge AA, Harrison PL. 2015. Ongoing unraveling of a continental fauna:

755   Decline and extinction of Australian mammals since European settlement. *Proceedings of*

756   *the National Academy of Sciences* 112: 4531–4540.

757   Yezerinac SM, Lougheed SC, Handford P. 1992. Measurement Error and Morphometric

758   Studies: Statistical Power and Observer Experience. *Systematic Biology* 41: 471–482.